Ultrasensitive terahertz sensing with high-*Q* Fano resonances in metasurfaces

Ranjan Singh,[1,2,a),b)] Wei Cao,[3,b)] Ibraheem Al-Naib,[4,b)] Longqing Cong,[1,2] Withawat Withayachumnankul,[5] and Weili Zhang[3,c)]
[1]*Division of Physics and Applied Physics, School of Physical and Mathematical Sciences, Nanyang Technological University, Singapore 637371*
[2]*Centre for Disruptive Photonic Technologies, School of Physical and Mathematical Sciences, Nanyang Technological University, Singapore 637371*
[3]*School of Electrical and Computer Engineering, Oklahoma State University, Stillwater, Oklahoma 74078, USA*
[4]*Department of Physics, Engineering Physics and Astronomy, Queen's University, Kingston, Ontario K7L 3N6, Canada*
[5]*School of Electrical and Electronic Engineering, The University of Adelaide, Adelaide, South Australia 5005, Australia*

(Received 9 July 2014; accepted 15 August 2014; published online 27 October 2014)

High quality factor resonances are extremely promising for designing ultra-sensitive refractive index label-free sensors, since it allows intense interaction between electromagnetic waves and the analyte material. Metamaterial and plasmonic sensing have recently attracted a lot of attention due to subwavelength confinement of electromagnetic fields in the resonant structures. However, the excitation of high quality factor resonances in these systems has been a challenge. We excite an order of magnitude higher quality factor resonances in planar terahertz metamaterials that we exploit for ultrasensitive sensing. The low-loss quadrupole and Fano resonances with extremely narrow linewidths enable us to measure the minute spectral shift caused due to the smallest change in the refractive index of the surrounding media. We achieve sensitivity levels of 7.75×10^3 nm/refractive index unit (RIU) with quadrupole and 5.7×10^4 nm/RIU with the Fano resonances which could be further enhanced by using thinner substrates. These findings would facilitate the design of ultrasensitive real time chemical and biomolecular sensors in the fingerprint region of the terahertz regime. © *2014 AIP Publishing LLC*. [http://dx.doi.org/10.1063/1.4895595]

The exotic properties of metamaterials have led to very novel effects in controlling the electromagnetic fields that have given rise to negative refraction, super lenses, invisibility cloaks, slow light effects, and subwavelength resolution imaging.[1–4] Although significant progress has been made in demonstrating these functionalities with smart metamaterial device designs, there are still fundamental roadblocks to their high efficiency performance which has restricted their widespread practical implementation. Low performance of metamaterial and plasmonic devices is mainly due to the radiative and the non-radiative losses encountered in these systems.[5] Recently, several schemes have been attempted to minimize the losses such as by introducing gain, by using low loss superconductors,[6] dielectric materials, or by optimizing the shape and size of the metallic subwavelength structure.[7–13]

Overcoming the losses would certainly enhance the performance of almost all metamaterial and plasmonic based devices. One of the significant device applications that plasmonic metamaterial has been proposed is that of a sensor at optical,[14–17] infrared,[18–22] and terahertz[23–32] frequencies. Ultrasensitive resonant sensing performance could be only achieved by high quality (Q) factor resonances that have extremely narrow linewidths and are easy to detect. Metamaterial structures have the unique advantage of being able to support resonances at any desired frequency based on their structural size, and these resonances are responsive to the changes in the effective index of refraction at their surface. As the Q factor of the metamaterial increases, the photon lifetime in the resonator increases that leads to enhanced field interaction with the sample on the surface. Metamaterials have the potential to be a great sensing platform since they could be easily fabricated on different types of flexible and thin substrates.[27,28] However, the losses in metamaterials limit their sensing performance as the low quality factor resonances typically lack the ability to detect small shifts in the resonance frequency due to the spectrally broad resonances.[27–30] Most of the previous works on metamaterial and plasmonic based sensing use the low Q resonances at terahertz, infrared, and optical frequencies.[11–17,25–33]

In this article, we have performed sensing using planar metasurfaces with an order of magnitude higher Q factors than previously demonstrated. Low loss, high-Q quadrupole, and Fano resonances are excited by breaking the symmetry of the metamaterial resonator structure, thus forming an asymmetric split ring resonator (ASR).[8–13,34,35] The higher Q resonances support strong interaction between the electromagnetic wave and a specific analyte. The sharp resonances of a low-loss high-Q metamaterial allow the detection of very small spectral shifts that occurs from the minute quantity of analyte interaction with the highly concentrated electric field in the split gaps of the meta-atoms. We demonstrate

a)Electronic mail: ranjans@ntu.edu.sg
b)R. Singh, W. Cao, and I. Al-Naib contributed equally to this work.
c)Electronic mail: weili.zhang@okstate.edu

terahertz (THz) domain refractive index sensing with high Q quadrupole resonance excited in one orientation and the high Q Fano resonance excited in the orthogonal orientation.[9] Terahertz sensing has received a lot of attention in recent times because of their significant scientific and technological potential in multidisciplinary fields.[36,37] Metasurfaces offer another important sensing platform at this frequency regime and there is a continued quest for enhancing the sensitivity of these planar devices.

A broadband terahertz time-domain spectrometer (THz-TDS) in transmission mode was used to characterize the sensing aspect of high-Q quadrupolar and Fano resonances.[9,38] The Gaussian beam of the terahertz pulse is focused to a beam waist of 3.5 mm for small sample characterization. The terahertz asymmetric split ring (TASR) metamaterial samples were fabricated on high-resistivity (4 kΩ cm), double-side polished, 0.5-mm-thick n-type silicon substrate using photolithography and a 200-nm-thick aluminum was thermally metallized to form the TASRs. A 10-mm-thick, high-resistivity (4 kΩ cm) silicon plate was placed in optical contact behind the metamaterial substrate to eliminate the Fabry Perot reflection from the back surface of the substrate that enabled a scan length of 200 ps with frequency resolution of 5 GHz. Figure 1(a) shows the microscopic image of the TASR array where the asymmetry in the TASR is introduced by displacing the lower gap from the central vertical axis with $d = 5\,\mu$m, where d represents the lower gap displacement from the center. The sample array size is 10 mm × 10 mm. The metamaterial sample is placed midway between the transmitter and receiver in the far-field at the focused beam waist, and the transmitted terahertz pulses were measured at normal incidence such that the electric and magnetic fields of the incident terahertz radiation are in the plane of the metasurface. Figure 1(b) shows the schematic of the quadrupole resonance current distribution for incident electric field along the x-axis and the corresponding excitation of a resonance with high-Q factor of 65 is shown in Fig. 1(d). The first order diffractive mode is matched with the quadrupole resonance in order to enhance the Q factor.[13,39–41] A different mode with anti-parallel current distribution, as shown in Fig. 1(c), typically known as the Fano resonance is excited with the incident electric field pointing towards the y-axis and the asymmetric line shaped resonance with Q factor of 28 is excited as shown in Fig. 1(e). Therefore, the planar TASR metamaterial used in this work is capable of supporting high-Q resonances for electric field in orthogonal directions enabling ultrasensitive sensing when an analyte layer is deposited on top of the TASR metasurface, as shown in Figs. 1(b) and 1(c). The corresponding red shift of quadrupole and Fano resonance frequencies could be clearly seen in Figs. 1(d) and 1(e).

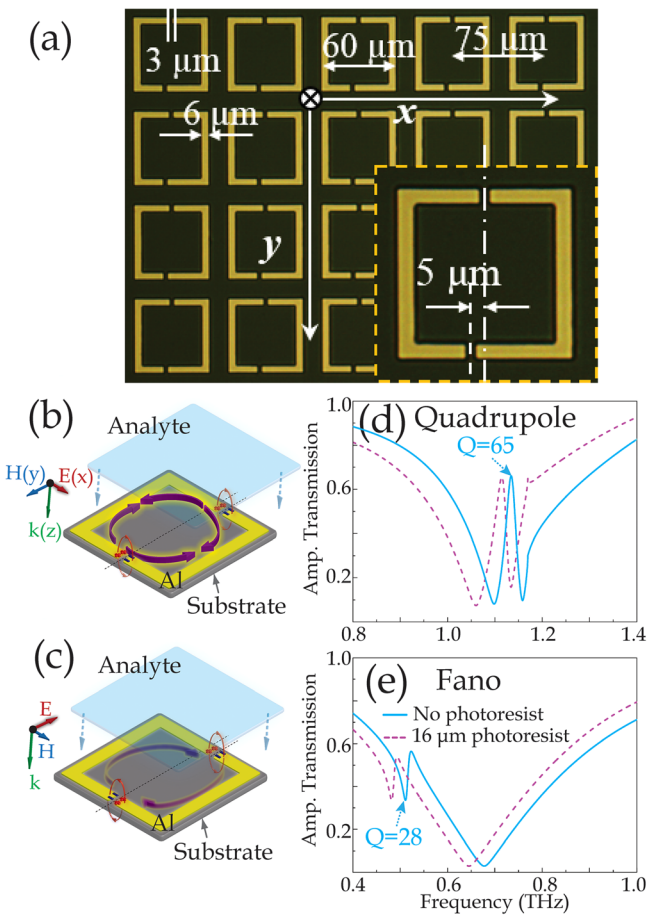

FIG. 1. (a) Microscopic image of the terahertz asymmetric split-ring (TASR) metamaterial array with the detailed geometric dimensions, (b) TASR unit cell where the quadrupole resonance is excited and the analyte photoresist layer is deposited on top of the metasurface, (c) TASR unit cell where the Fano resonance is being excited, (d) the transmission spectra of the quadrupole resonance with and without the analyte layer, and (e) transmission spectra of the Fano resonance with and without the analyte layer.

Different thicknesses of photoresist were spun coated on the planar TASR sample. Figure 2(a) shows the simulated transmission response of the metasurface where we observe gradual red shifting of the quadrupole resonance with increasing thickness of the photoresist overlayer as the analyte. The red shift of quadrupole resonance for film thicknesses 1, 4, 8, and 16 μm is 8.38, 14.53, 17.41, and 19.5 GHz, respectively, when compared with the quadrupole resonance frequency without any analyte layer on top of the metasurface, i.e., 1.13 THz. Figure 2(b) shows the measured data which agree well with the high resolution frequency domain simulations performed with CST Microwave Studio. The refractive index of

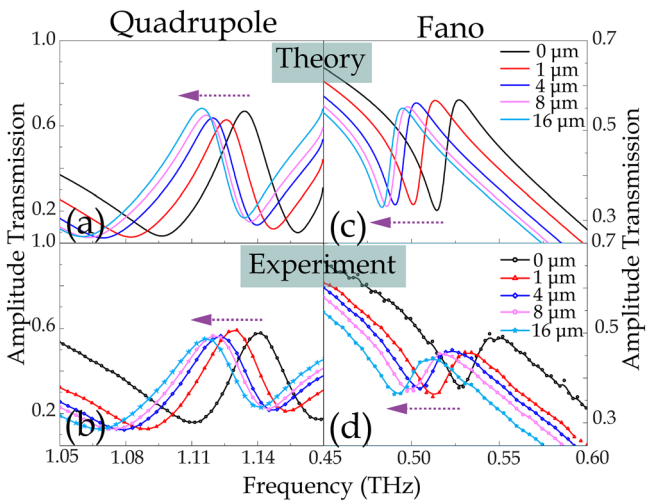

FIG. 2. (a) Calculated and (b) measured transmission spectra of quadrupole resonance with different thicknesses of photoresist coating on the metasurface. (c) Calculated and (d) measured transmission spectra of Fano resonance with different thicknesses of photoresist coating on the metasurface.

the spin coated photoresist is $n = 1.6$. The largest red shift occurs for the first 1 μm thickness of photoresist. Figure 1(b) shows current distribution of the quadrupole resonance mode where the pairs of diagonally anti parallel currents ensure extremely low radiation losses. We would later discuss the electric field distribution of the quadrupole mode and observe the strong fields excited at this resonance in the TASR structure. The red shift is mainly caused by the increase in the capacitance of the TASR split gaps. The dielectric photoresist analyte fills the split gaps and also leads to the enhancement of electric field in the TASR capacitive split gaps.

The metasurface samples were also measured for the orthogonal (y-axis) direction excitation. For this orientation, we excite an asymmetric line shaped Fano resonance at 0.52 THz (without analyte). For overlayer thicknesses of 1, 4, 8, and 16 μm, the corresponding red shift of the Fano resonance is 10, 21.3, 26.1, and 29 GHz, respectively, as shown in Fig. 2(c), which represents the simulated transmission spectra. Figure 2(d) is the measured transmission spectra which agreed well with the simulated data. The largest degree of redshift in the Fano resonance frequency was once again for the first overlayer coating of 1 μm. The total shift of 29 GHz for 16 μm thickness analyte is significantly higher than the total shift (19.5 GHz) in case of quadrupole resonance. This highlights the higher sensitivity of the Fano resonance over the quadrupolar resonance, which we would discuss in detail later. Figure 1(c) shows the antiparallel current directions in the TASR at the Fano resonance frequency. The antiparallel current distribution is key to reduced radiation losses in the structure and it also facilitates a very weak coupling with the free space.

In order to understand the redshift of the quadrupole and the Fano resonances, we numerically simulated the electric fields at the corresponding resonances with and without the dielectric analyte overlayer on top of the metasurface. Column 1 in Fig. 3 reveals the field distribution at various resonances without any analyte and column 2 shows the field at the corresponding shifted resonances with 16 μm photoresist overlayer. Figures 3(a), 3(c), and 3(e) show the electric field in TASR at different frequencies when the incident terahertz field is along the x-axis. In Fig. 3(a), we see the fields at the quadrupole resonance peak at 1.13 THz. A closer observation clearly reveals the four nodes in the field distribution due to which we define the resonance as the quadrupolar mode. In the adjacent Fig. 3(b), the electric fields in the two split gaps become stronger compared to that in Fig. 3(a) due to the 16 μm analyte dielectric layer. The dielectric analyte supports the field enhancement as it occupies the volume in the split gap on top as well as bottom arm of TASR that acts as dual capacitors in each unit cell. Figure 3(c) shows the electric field at the first resonance dip (at 1.096 THz) for the x axis excitation and we could notice that the longer right side arm of the TASR is excited with two distinct electric field nodes, thus acting as a dipolar resonant excitation. Similarly, in Fig. 3(e), the simulated electric field is at the second resonance dip (1.158 THz) at which only the left hand side shorter metallic arm of TASR is excited with two observable nodes. Both of these resonance dips are dipolar excitations individually in each of the metallic wire arm that forms the TASR. The corresponding red shifted resonant

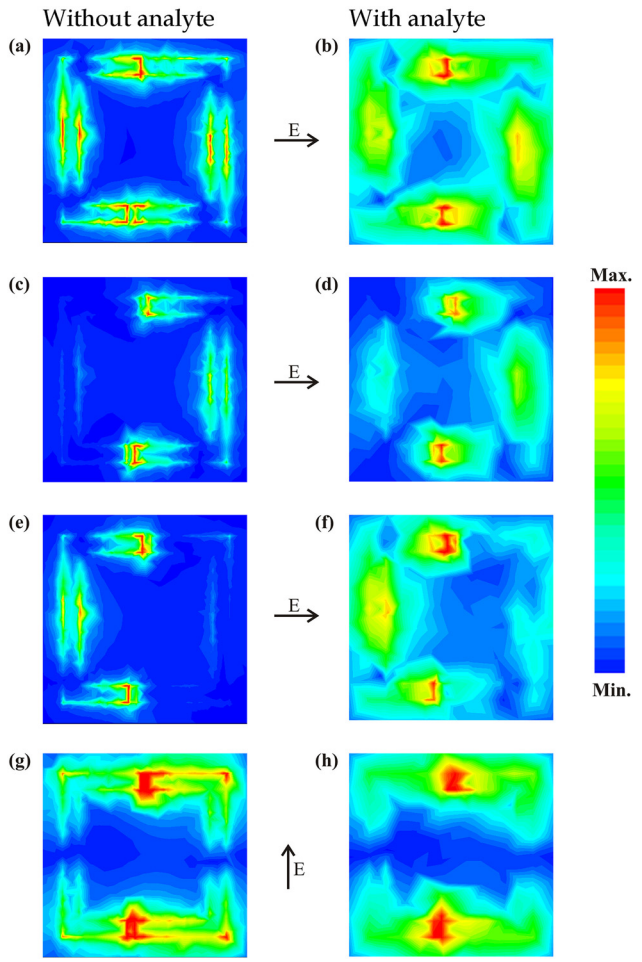

FIG. 3. Simulated electric field distribution at (a) and (b) 1.13 THz, quadrupole resonance peak, (c) and (d) 1.096 THz, dipole resonance dip, (e) and (f) 1.158 THz, dipole resonance dip, and (g) and (h) 0.515 THz, Fano resonance dip with 0 μm and 16 μm analyte overlayer thickness coated on the metasurface.

electric fields with 16 μm overlayer have been shown in Figs. 3(d) and 3(f), respectively, where we clearly observe field enhancement at the edges of each metallic wire for the dipolar excitations.

After probing the two resonance dips and the single peak of the quadrupole resonance, we looked at the response of the TASR metasurface for the orthogonal excitation (with E along the y axis) and investigated the electric field at the dip of the Fano resonance at 0.515 THz, as shown in Fig. 3(g). With a closer look at the fields, it appears that at the Fano resonance their intensity in the split gaps of TASR is much stronger compared to that of the quadrupolar resonance. This observation is a key in understanding that these tightly confined fields at the Fano resonance excitation are extremely sensitive to its surroundings, thus we obtain significantly higher red shift of the resonance than that compared to the quadrupolar resonances. As it could be seen in Fig. 3(h), the field confinement is further enhanced at the Fano resonance with the dielectric analyte layer on top of the metasurface.

Since the change in the resonance frequency of quadrupole and the Fano resonances was different for the same thickness of coated analyte on the metasurface, we analyzed the sensitivity of both resonances for identical of thickness

of the analyte layer and by varying the refractive index of the analyte. Figure 4(a) shows the shift in the quadrupole resonance with a constant thickness of 4 μm but different refractive index of the analyte. The total shift in the quadrupole resonance frequency by changing the refractive index of analyte from $n=1$ to $n=1.6$ is found to be 15 GHz. We repeated the process for the Fano resonance, as shown in Fig. 4(b), and the total shift in this case is observed to be 22 GHz. We plotted the resonance shift versus the change in refractive index of the analyte for a constant thickness of 4 μm in Fig. 4(c) and estimated the sensitivity of both resonances. The quadrupole and Fano resonance sensitivities turned out to be 23.9 and 36.7 GHz/refractive index unit (RIU), respectively. We converted these numbers into $\Delta\lambda$/RIU by using $|\frac{d\lambda}{dn}| = \frac{c}{f_0^2} * \frac{df}{dn}$, where "$c$" is the speed of light, f_0 is resonance frequency, and n represents the refractive index of the analyte. In terms of $\Delta\lambda$/RIU, the corresponding sensitivities that we obtained for the 4 μm thick analyte with quadrupole and Fano resonances are 5.62×10^3 nm/RIU and 4.23×10^4 nm/RIU, respectively. These sensitivity values are higher than previously reported sensitivities using planar metamaterial structures on similar thickness substrates.[29–32]

We further investigated the analyte thickness dependent sensitivity of the TASR metasurface through rigorous simulations as shown in Fig. 5(a). We observe that the sensitivities of both the resonances increase exponentially with the increasing analyte thickness and eventually saturate at about 16 μm thickness highlighting that the electric fields extend up to 16 μm in the dielectric analyte coated on top of the metasurface layer. We also notice that the Fano resonance has significantly higher sensitivity than the quadrupole resonance which saturates at a lower value of maximum sensitivity. The maximum sensitivities are found to be 5.7×10^4 nm/RIU (49.3 GHz/RIU) for the Fano resonance and 7.75×10^3 nm/RIU (33 GHz/RIU) for the quadrupole resonance with analyte thickness of 16 μm. The difference in maximum sensitivities of the two resonances can be attributed to the different electric field mode profiles in the capacitive gaps of the TASR at the respective resonance frequencies. A straightforward approach to further enhance the sensitivity of the TASR metasurfaces would be to use ultrathin substrates, since it would allow stronger interaction of analyte with the intense field in the capacitive gaps that otherwise remains mostly confined in the thick substrates. Thus, we probed the sensitivities of both resonances at varying thicknesses of the silicon substrate in our simulation model. The analyte coated on the metasurface has a fixed thickness of 1 μm with a refractive index varying from $n=1$ to $n=1.6$. We found that the metasurface becomes

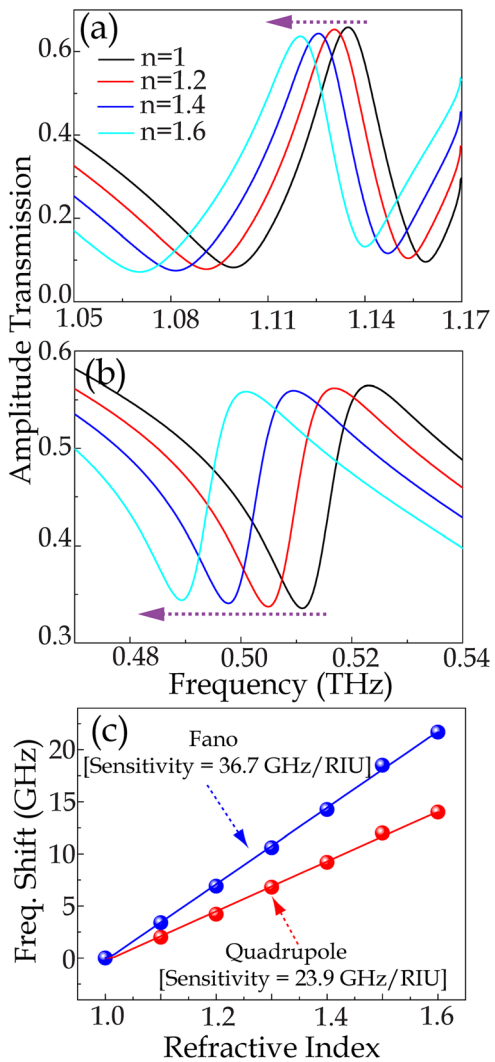

FIG. 4. Simulated amplitude transmission spectra of (a) quadrupole resonance and (b) Fano resonances when 4 μm constant thickness analyte with different refractive indices is coated on the metasurface. (c) Quadrupole and Fano resonances shift with the change in refractive indices.

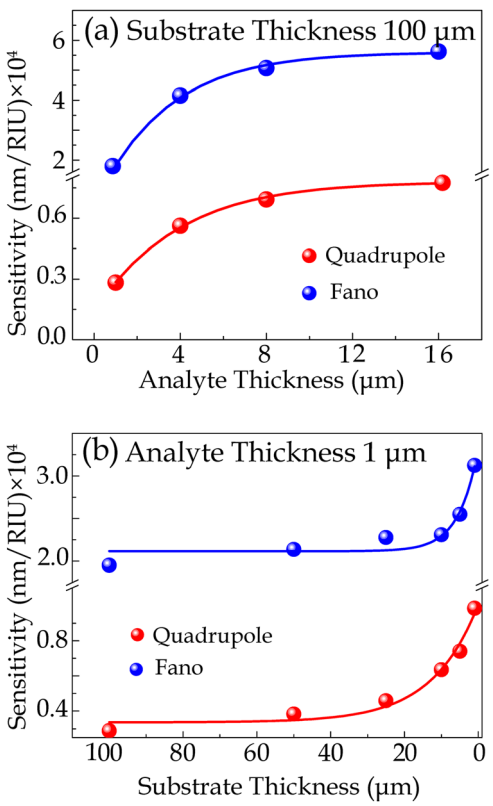

FIG. 5. Simulated sensitivities of Fano and quadrupole resonances with (a) different analyte thicknesses with varying refractive indices were coated on metasurface on 100 μm thick silicon substrate and (b) 1 μm thick analyte of varying refractive indices at decreasing thicknesses of silicon substrate. The solid curves represent exponential fits to the data points in (a) and (b).

extremely sensitive to both resonances below substrate thickness of 20 μm as shown in Fig. 5(b). The sensitivity of Fano resonance gets enhanced by a factor of two and of the quadrupole resonance by a factor of three for 1 μm thick analyte. This occurs due to much stronger interaction of analyte layer with the enhanced electric field in the capacitive gaps of the metasurface on ultrathin substrates at both resonances. However, we would like to stress that Fano resonances continue to be more sensitive than the quadrupolar modes even in the ultrathin substrates due to strong Fano mode confinement. Thus, thinner substrates enable a further enhancement in the sensitivities of the high-Q resonances in metasurfaces. Thinner substrates offer a new avenue to apply flexible non-planar surfaces in designing novel ultrasensitive sensors.

In summary, we have demonstrated high-Q ultrasensitive sensing via strong light-matter interaction at the ultra-sharp quadrupole and Fano resonances in the fingerprint terahertz spectral domain. High resolution terahertz measurements allowed us to measure the minute shift in the resonance frequencies as thin layers of analyte bonded with the metasurface. The sensitivities achieved by using the high-Q resonant metasurfaces in this work outperform other schemes based on low Q Lorentzian planar metamaterial and plasmonic structures. We believe that the impact of our results lies in identifying high-Q terahertz metasurface based ultrasensitive sensing that would open up avenues for advanced design and realization of real time on-chip chemical and bio molecular detection with spectral signatures in the terahertz regime.

We would like to acknowledge funding from NTU startup Grant No. M4081282 and U.S. NSF grant.

[1]V. M. Shalaev, Nat. Photonics **1**(1), 41–48 (2007).
[2]C. M. Soukoulis, M. Kafesaki, and E. N. Economou, Adv. Mater. **18**(15), 1941–1952 (2006).
[3]N. I. Zheludev and Y. S. Kivshar, Nat. Mater. **11**(11), 917–924 (2012).
[4]Y. Liu and X. Zhang, Chem. Soc. Rev. **40**(5), 2494–2507 (2011).
[5]A. Boltasseva and H. A. Atwater, Science **331**(6015), 290–291 (2011).
[6]R. Singh and N. Zheludev, Nat. Photonics **8**, 679–680 (2014).
[7]S. Xiao, V. P. Drachev, A. V. Kildishev, X. Ni, U. K. Chettiar, H.-K. Yuan, and V. M. Shalaev, Nature **466**(7307), 735–738 (2010).
[8]V. Fedotov, M. Rose, S. Prosvirnin, N. Papasimakis, and N. Zheludev, Phys. Rev. Lett. **99**(14), 147401 (2007).
[9]W. Cao, R. Singh, I. A. Al-Naib, M. He, A. J. Taylor, and W. Zhang, Opt. Lett. **37**(16), 3366–3368 (2012).
[10]R. Singh, I. Al-Naib, W. Cao, C. Rockstuhl, M. Koch, and W. Zhang, IEEE Trans. Terahertz Sci. Technol. **3**(6), 820 (2013).
[11]I. Al-Naib, R. Singh, C. Rockstuhl, F. Lederer, S. Delprat, D. Rocheleau, M. Chaker, T. Ozaki, and R. Morandotti, Appl. Phys. Lett. **101**(7), 071108 (2012).
[12]R. Singh, I. A. Al-Naib, M. Koch, and W. Zhang, Opt. Express **19**(7), 6312–6319 (2011).
[13]R. Singh, I. A. Al-Naib, Y. Yang, D. R. Chowdhury, W. Cao, C. Rockstuhl, T. Ozaki, R. Morandotti, and W. Zhang, Appl. Phys. Lett. **99**(20), 201107 (2011).
[14]J. N. Anker, W. P. Hall, O. Lyandres, N. C. Shah, J. Zhao, and R. P. Van Duyne, Nat. Mater. **7**(6), 442–453 (2008).
[15]B. Lahiri, A. Z. Khokhar, R. M. De La Rue, S. G. McMeekin, and N. P. Johnson, Opt. Express **17**(2), 1107–1115 (2009).
[16]N. Liu, M. L. Tang, M. Hentschel, H. Giessen, and A. P. Alivisatos, Nat. Mater. **10**(8), 631–636 (2011).
[17]N. Papasimakis, Z. Luo, Z. X. Shen, F. De Angelis, E. Di Fabrizio, A. E. Nikolaenko, and N. I. Zheludev, Opt. Express **18**(8), 8353–8359 (2010).
[18]E. Cubukcu, S. Zhang, Y.-S. Park, G. Bartal, and X. Zhang, Appl. Phys. Lett. **95**(4), 043113 (2009).
[19]N. Liu, T. Weiss, M. Mesch, L. Langguth, U. Eigenthaler, M. Hirscher, C. Sönnichsen, and H. Giessen, Nano Lett. **10**(4), 1103–1107 (2010).
[20]C. Wu, A. B. Khanikaev, R. Adato, N. Arju, A. A. Yanik, H. Altug, and G. Shvets, Nat. Mater. **11**(1), 69–75 (2011).
[21]J. Zhao, C. Zhang, P. V. Braun, and H. Giessen, Adv. Mater. **24**(35), OP247–OP252 (2012).
[22]Y. Yang, I. I. Kravchenko, D. P. Briggs, and J. Valentine, "High quality factor Fano-resonant all-dielectric metamaterials," preprint arXiv:1405.3901 (2014).
[23]I. A. I. Al-Naib, C. Jansen, and M. Koch, Appl. Phys. Lett. **93**(8), 083507 (2008).
[24]C. Debus and P. H. Bolivar, Appl. Phys. Lett. **91**(18), 184102 (2007).
[25]T. Driscoll, G. Andreev, D. Basov, S. Palit, S. Cho, N. Jokerst, and D. Smith, Appl. Phys. Lett. **91**(6), 062511 (2007).
[26]B. Ng, S. Hanham, V. Giannini, Z. Chen, M. Tang, Y. Liew, N. Klein, M. Hong, and S. Maier, Opt. Express **19**(15), 14653–14661 (2011).
[27]H. Tao, L. R. Chieffo, M. A. Brenckle, S. M. Siebert, M. Liu, A. C. Strikwerda, K. Fan, D. L. Kaplan, X. Zhang, and R. D. Averitt, Adv. Mater. **23**(28), 3197–3201 (2011).
[28]H. Tao, A. C. Strikwerda, M. Liu, J. P. Mondia, E. Ekmekci, K. Fan, D. L. Kaplan, W. J. Padilla, X. Zhang, and R. D. Averitt, Appl. Phys. Lett. **97**(26), 261909 (2010).
[29]W. Withayachumnankul, H. Lin, K. Serita, C. M. Shah, S. Sriram, M. Bhaskaran, M. Tonouchi, C. Fumeaux, and D. Abbott, Opt. Express **20**(3), 3345–3352 (2012).
[30]J. F. O'Hara, R. Singh, I. Brener, E. Smirnova, J. Han, A. J. Taylor, and W. Zhang, Opt. Express **16**(3), 1786–1795 (2008).
[31]S.-Y. Chiam, R. Singh, W. Zhang, and A. A. Bettiol, Appl. Phys. Lett. **97**(19), 191906 (2010).
[32]S.-Y. Chiam, R. Singh, J. Gu, J. Han, W. Zhang, and A. A. Bettiol, Appl. Phys. Lett. **94**(6), 064102 (2009).
[33]L. Cong and R. Singh, "Sensing with THz metamaterial absorbers," preprint arXiv:1408.3711 (2014).
[34]B. Luk'yanchuk, N. I. Zheludev, S. A. Maier, N. J. Halas, P. Nordlander, H. Giessen, and C. T. Chong, Nat. Mater. **9**(9), 707–715 (2010).
[35]A. E. Miroshnichenko, S. Flach, and Y. S. Kivshar, Rev. Mod. Phys. **82**(3), 2257 (2010).
[36]M. Tonouchi, Nat. Photonics **1**(2), 97–105 (2007).
[37]B. Ferguson and X.-C. Zhang, Nat. Mater. **1**(1), 26–33 (2002).
[38]D. Grischkowsky, S. Keiding, M. V. Exter, and C. Fattinger, J. Opt. Soc. Am. B **7**(10), 2006–2015 (1990).
[39]R. Singh, C. Rockstuhl, and W. Zhang, Appl. Phys. Lett. **97**(24), 241108 (2010).
[40]R. Singh, I. A. Al-Naib, M. Koch, and W. Zhang, Opt. Express **18**(12), 13044–13050 (2010).
[41]I. Al-Naib, C. Jansen, R. Singh, M. Walther, and M. Koch, IEEE Trans. Terahertz Sci. Technol. **3**, 772–782 (2013).